Flinders UNIVERSITY

Non-toxic luminescent carbon dot/poly(dimethylacrylamide) nanocomposite reagent for latent fingermark detection synthesized via surface initiated RAFT polymerization

Jessirie Dilag[1, 2], Hilton Kobus[3], Yang Yu[1], Christopher T. Gibson[1] and Amanda V. Ellis[1*]

[1] Flinders Centre for Nanoscale Science and Technology, Flinders University, Sturt Road, Bedford Park SA, Australia, 5042

[2] Centre for Forensic Science, University of Technology, Sydney, Broadway, Ultimo NSW, 2007

[3] School of Chemical and Physical Sciences, Flinders University, Sturt Road, Bedford Park, SA, Australia, 5042

***Corresponding Author**

Prof. Amanda Ellis

amanda.ellis@flinders.edu.au

Keywords

Nanoparticle, carbon, fingermark detection, RAFT polymerization, forensic science

ABSTRACT

Here, non-toxic luminescent carbon nanoparticles, namely carbon dots (C-dots), were facilely synthesized via a one pot hydrothermal route. Raman, Fourier transform infra-red, fluorescence, carbon nuclear magnetic resonance and X-ray photoelectron spectroscopies revealed the carbon dots possessed a graphitic-like core with an oxidized surface. The oxidized surface of the C-dots allowed for functionalization of the C-dots with 2-methyl-2-[(dodecylsulfanylthiocarbonyl)sulfanyl]propanoic acid chain transfer agent (C_{12} CTA). Poly(*N*,*N*-dimethylacrylamide) (p(DMA)) was then grafted-from the graphene surface via surface initiated reversible addition fragmentation chain transfer (RAFT) polymerization. The resulting luminescent carbon dot-polymer nanocomposite, C-dot/p(DMA), was analysed using UV-visible and fluorescence spectrometry verifying that the functionalized surface was responsible for the C-dots' luminescence. This C-dot/p(DMA) nanocomposite was water soluble and was used as solution for the luminescent detection of latent fingermarks deposited on non-porous aluminium foil substrates.

INTRODUCTION

Fingermark detection in forensic sciences is an indispensable source of evidence for identification purposes. Current attempts to improve the visualization of latent fingermarks are often driven towards luminescent enhancement or detection to obtain optimum contrast between the detected latent fingermark and the surface. With current advances in nanoscience and nanotechnology there has been a drive towards the synthesis and application of fluorescent quantum dots (QDs) in fingermark reagents [1-7]. QDs exhibit extraordinary optical and electrical properties making them a desirable component to integrate into these reagents. However, they are conventionally made up of toxic metals, in particular cadmium, the most common being cadmium sulfide (CdS) and cadmium selenium (CdSe) QDs [1-11]. This work describes a non-toxic approach in which nano-carbons are used, in particular, luminescent carbon nanoparticles called carbon dots (C-dots) [12-35].

C-dots differ from other carbon nanomaterials such as fullerenes, graphene or nanodiamonds in the amount of graphitic structure or sp^2 character and the degree of oxidation [14]. Interestingly, the source of C-dot fluorescence emission differs from graphene QDs and nanodiamonds. In the case of nanodiamonds and graphene QDs, radiative processes occur within the graphitic core with π-π^* electronic transfers whereas with C-dots there is developing evidence that fluorescence emission arises from radiative processes occurring at the surface – as a result of oxidation or surface passivation [12-14]. Oxidation of the surface leaves the surface of the C-dots decorated with oxygen containing functional groups such as COOH, C-OH and C=O. In particular, it is suggested that the COOH groups are responsible for C-dot luminescent behaviour under UV illumination [12-14, 20-22]. Surface oxidation of C-dots comes about from the synthesis route selected, whether it is from a top down approach (e.g. laser ablation [18]) or bottom up approach (e.g. microwave [23] and hydrothermal reactions under acidic conditions [24-32]). Liu et al. [31] use a hydrothermal reaction to

produce C-dots. First, soot was collected by placing a piece of aluminium foil or glass plate on top of a burning candle. The soot was then refluxed under acidic conditions (5 M HNO_3) over night, cooled and isolated via centrifugation, dialysis and polyacrylamide gel electrophoresis (PAGE) fractionation. Following this Ray et al. [25] refluxed candle soot under acidic conditions (5 M HNO_3) for 12 h. They found that if the carbon soot was refluxed for less than 12 h, this resulted in a smaller C-dot yield. However, refluxing for longer than 12 h gave no appreciable gain in C-dot yield [33]. Other sources of carbon have been used including refluxing orange juice [26], bread, and sugar [32].Post-functionalization of C-dots makes them available to a broad range of applications. In particular, C-dots have been explored for applications where QDs have initially been researched such as bio-imaging. However to date the use of C-dots in fingermark detection has not been reported [14, 22, 25]. A synthetic route previously reported by our group synthesized CdS QD based fingermarks reagents [6]. The experimental procedure involved reversible addition fragmentation chain transfer (RAFT) polymerization, enabling surface functionalization under mild conditions.

Here, we fabricate C-dots from the hydrothermal treatment of activated charcoal (AC) under acidic conditions, and subsequently conjugate the pendant OH groups on the C-dot surface to carboxyl terminated chain transfer agent, 2-methyl-2-[(dodecylsulfanylthiocarbonyl)sulfanyl]propanoic acid (C_{12} CTA) via Steglich esterification. Surface initiated RAFT polymerization of *N*,*N*-dimethylacrylamide (DMA) from the surface of the C-dot/C_{12} CTA, resulted in water soluble luminescent C-dot/p(DMA) nanocomposites. DMA was selected due to its organic adhesive properties as a gel, transparency and its solubility in water. An aqueous C-dot/p(DMA) based fingermark reagent was prepared and used to visually detect charged latent fingermarks that had been deposited onto non-porous aluminum foil substrates and was visualized, and photographed, under UV illumination (via the Polilight® - a forensic light source).

Materials

Acetone (AR grade), 2-2′-azobis(isobutyronitrile) (AIBN), Activated charcoal (AC), aluminum oxide (basic), deuterated chloroform ($CDCl_3$), deuterated dimethylsulfoxide (d-DMSO) diethyl ether (anhydrous), magnesium sulfate ($MgSO_4$), *N*,*N*-dimethylacrylamide (DMA, purity: 99%, with 500 ppm monomethyl ether hydroquinone inhibitor), *N*,*N*′-dicyclohexylcarbodiimide (DCC), 4-dimethylaminopyridine (DMAP), anhydrous *N*,*N*-dimethylformamide (DMF), nitric acid (HNO_3, purity: 70%), sulfuric acid (H_2SO_4), styrene (Sty, 99%, with 4-tert-butylcatechol as stabilizer), and anhydrous toluene, were purchased from Sigma Aldrich, Australia. 2-methyl-2-[(dodecylsulfanylthiocarbonyl)sulfanyl]propanoic acid (C_{12} CTA) was purchased from STREM chemical Inc., USA. Acetone (HPLC Grade) was purchased from Chem-Supply, Australia. All water used was Milli-Q water (18.2 MΩ cm^{-1}).

EXPERIMENTAL

Synthesis of C-dots via the one-pot hydrothermal route

Activated charcoal (1 g) and nitric acid (4 M, 100 mL) were stirred with a magnetic stir bar in a 200 mL round bottom flask under reflux, for 24 h. The solution was then filtered by gravity through filter paper (100 mm, 20-25 μm Whatman© paper) to remove any unreacted activated charcoal. The acidic filtrate of C-dots was then neutralized using NaOH (4 M).

The neutralization by-product ($NaNO_3$) was recrystallized (via water evaporation and cooling the solution) and removed via gravity filtration through filter paper (100 mm, 20-25 μm Whatman© paper). DMF (50 mL) was added to the filtered aqueous C-dots solution and the solution was distilled to remove the excess water. After cooling, the solution was dried using anhydrous $MgSO_4$ (c.a. 2 g). This resulted in C-dots dispersed in DMF.

Surface functionalization of C-dots with C_{12} CTA via Steglich esterification

DMAP (10 mg), C_{12} CTA (20 mg) and C-dots in DMF (50 mL) were stirred with a magnetic stir bar in a 100 mL round bottom flask for 80 min at 0 °C under nitrogen. DCC (20 mg in 5 mL DMF) was then added to the solution drop-wise over a 2 min time period. The solution was then left to stir, under nitrogen at room temperature for 48 h. Any undesirable by-product from the DCC/DMAP coupling reaction (e.g., *N*,*N*′-dicyclohexylurea, a white precipitate) was removed via gravity filtration through filter paper (100 mm, 20-25 μm Whatman© paper).

Synthesis of C-dot/p(DMA) via surface initiated RAFT polymerization

DMA (5 mL), AIBN initiator (10 mg) and C-dots/C_{12} CTA in DMF (50 mL) were placed into a 100 mL glass vessel with a magnetic stir bar and sealed (with a rubber septum and copper wire). This solution was then degassed under nitrogen via syringe for 1 h before placing in a silicon oil bath with a stable temperature set at 60 °C, for 48 h. The polymerized solution was allowed to cool to room temperature before purifying via precipitation in excess cold diethyl ether (400 mL) to give C-dots/p(DMA). ^{1}H NMR ($CDCl_3$) δ (ppm) 0.98-1.20 (C-CH_3), 1.62 (CH_2), 2.12 (OC-CH), 2.71 (N-CH_3), 3.21 (S-CH_2) and 10.23 (C-COOH) [34].

Characterization

Particle size analysis by dynamic light scattering (DLS) was performed using a Malvern High Performance Particle Sizer HPPS-HPP5001 with a water dispersant refractive index and viscosity set to 1.5900 and 0.8872 cP, respectively. XPS survey analysis of the carbon and oxygen peaks were performed on a Leybold LHS-10 XPS spectrometer equipped with a monochromatic Al Kα source (1486.6 eV). The X-ray source was operated at 13 kV, 20 mA. Raman spectra were collected with a WiTEC alpha300R Microscope using a 40x objective

(Numerical Aperture 0.6) and 532 nm (E_{laser} = 2.33 eV). Raman spectra were recorded with typical integrations times between 10 to 20 s and 3 accumulations. Solution ^{13}C NMR data of all C-dot samples were recorded on a 600 MHz Bruker Advance NMR Spectrometer. ^{1}H nuclear magnetic resonance (NMR) spectra were recorded using a Bruker 400 MHz NMR spectrometer installed with Bruker TOPSHIM 2.1. For kinetic studies toluene was used as an internal standard. Fourier transform infra-red (FTIR) analysis was performed on a Thermo Electron FTIR spectrometer (Nicolet Avatar 370 PTGS Model). Thermogravimetric analysis (TGA) was performed using- a Thermal Advantage (TA) Hi-Res modulated TGA 2950 Thermogravimetric Analyser. A nitrogen flow rate of 50 mL min^{-1}, with a temperature range of 30–600 °C, at a 10 °C min^{-1} ramp rate was used. Gel permeation chromatography (GPC) was performed on a Shimazdu HPLC with a Varian PolarGel™ Organic GPC column (300 mm length, 7.5 mm) with a refractive index detector, and THF solvent (HPLC grade). Calibration of molecular mass was performed using PolarGel™ polystyrene standards. Polymer samples were prepared by cleaving the p(DMA) from the C-dot surface with H_2SO_4 treatment and precipitation into excess diethyl ether before re-dissolving sample in THF solvent for analysis. UV–visible spectra were recorded on a Varian 50 Spectrophotometer and fluorescence emission spectra were recorded on a Varian Cary Eclipse Fluorescence Spectrophotometer. An excitation of 350 nm was used in all cases. Quantum yield (QY) values were calculated with a calibration method against Rhodamine 6g (R6G) dye standards in H_2O.

Fingermark treatment and development

Charged latent fingermarks were prepared by the participant (female, age 27) rubbing the palmer side of the fingertips on the forehead, neck and shoulders before randomly pressing their fingers onto aluminum foil substrates (Black & Gold brand, Australia). Half the

fingermark bearing substrates were developed within 2 h of deposition whereas the other half were left to age for one week at room temperature and exposed to air before development.

An aqueous solution of the C-dot/p(DMA) nanocomposite (150 mg in 100 mL water) was prepared. Aluminum foil substrates bearing the latent fingermarks were immersed into the aqueous C-dot/p(DMA) with the fingermarks facing upwards. The substrates sunk to the bottom of the immersion tray and were left to sit in the nanocomposite solution for 5 s. After which time, the substrates were removed and washed with Milli-Q water (100 mL) to remove any excess nanocomposite. A Polilight Pl10 (Rofin, Australia) with an UV light (350 nm) excitation was used to visualize and photograph the developed fingermarks. Photographs were taken using a Nikon D3100 digital SLR camera with a 58 mm lens. A red (610 ± 40 nm) and a green filter (555 ± 24 nm) were used on the camera.

RESULTS AND DISCUSSION

Characterization of pristine C-dots

The average size of the C-dots was determined to be 8.7 nm ± 0.5 nm using dynamic light scattering (DLS) techniques. Raman spectroscopy was used to investigate and verify the crystalline nature and degree of sp^2 hybridization and hence graphitic, or diamond-like structure, of the C-dots with respect to its carbon precursor, AC. Figure 1 shows the stacked Raman spectra of AC and C-dots, respectively.

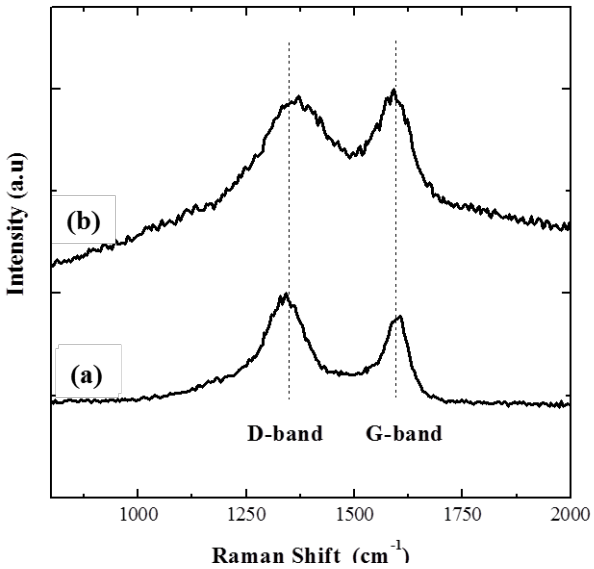

Figure 1. Stacked Raman spectra of (a) AC and (b) C-dots

Both the AC (Figure 1 (a)) and the C-dots (Figure 1 (b)) show the D-band relating to edge defects at 1320 cm^{-1}, as well as the G-band relating to the in-plane vibration of sp^2 carbon observed at 1590 cm^{-1} [35]. The ratio of intensities of these bands (I_D/I_G) was used to correlate the structural properties of the carbon. The I_D/I_G calculated for the AC was 1.16 and is higher than that for the C-dots at 1.01. This indicates that the structure of the C-dots is more nano-crystalline, as the vibrations of sp^2 carbon (G-band) are larger. In addition, a larger background in the Raman spectrum of the C-dots (Figure 1(b)) was observed, demonstrating the fluorescence emission by the nanoparticles under the Raman laser excitation (532 nm) [16, 36].

XPS analysis was performed to investigate the surface oxidation of the C-dots after HNO_3 treatment of the precursor, AC. Figure 2 (a) and (b) shows the XPS survey scans taken of AC and C-dots, respectively. The peak positions, peak area (%), full width half maximum (FWHM), and relative atomic concentrations (At %) are shown in Table 1.

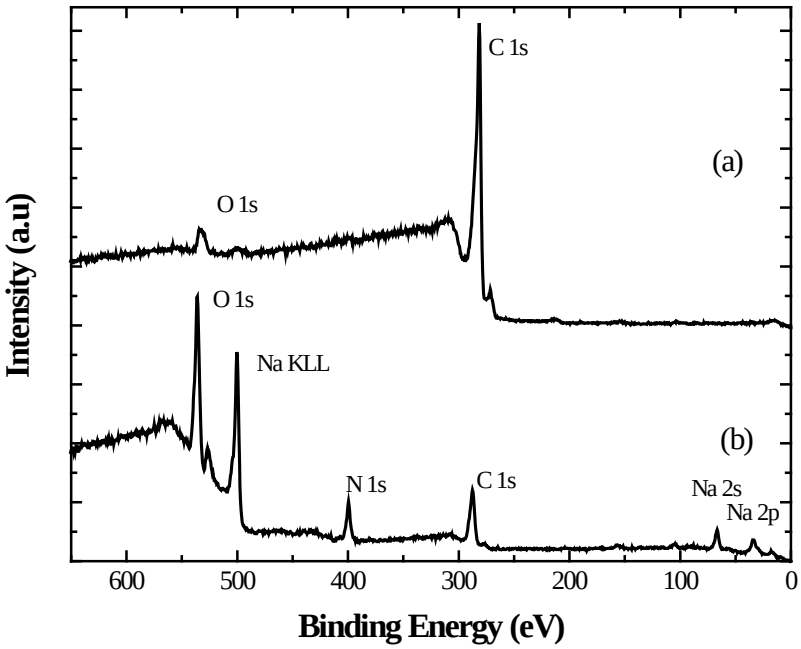

Figure 2. XPS survey scans of (a) AC and (b) purified C-dots.

Table 1. Peak position, peak area (%), FWHM and At % values calculated from the XPS analysis of (a) AC and (b) C-dots.

	Sample	**Peak Position (eV)**			**Peak area (cps.eV)**	**FWHM (eV)**	**At %**
(a)	AC	O	1s	532.5	1.3	7.1	3.7
		C	1s	281.5	11.6	4.1	96.3
(b)	C-dots	O	1s	532.5	2.4	3.8	28.7
		C	1s	287.5	4.1	5.0	21.6
		N	1s	399.1	1.4	3.0	7.3
		Na	KLL	507.5	7.2	3.7	37.9
			2s	63.2	0.64	3.6	3.2
			2p	31.8	0.24	4.0	1.3

Table 1 shows that the oxygen content (w.r.t carbon) increased dramatically when the AC (O content of 3.7 % w.r.t C) was transformed into C-dots (O content of approximately 56 % w.r.t. C). This confirmed the surface oxidation of the C-dots. The Na and N peaks are attributed to the $NaNO_3$ salt by product.

In order to further confirm the degree of sp^2 hybridization and type of surface oxidization ^{13}C NMR and FTIR spectroscopy were performed (Figure 3 (i) and (ii), respectively). Figure 3 (i) shows the ^{13}C NMR spectrum of the C-dots suspended in D_2O. AC is not shown as it is insoluble in all solvents.

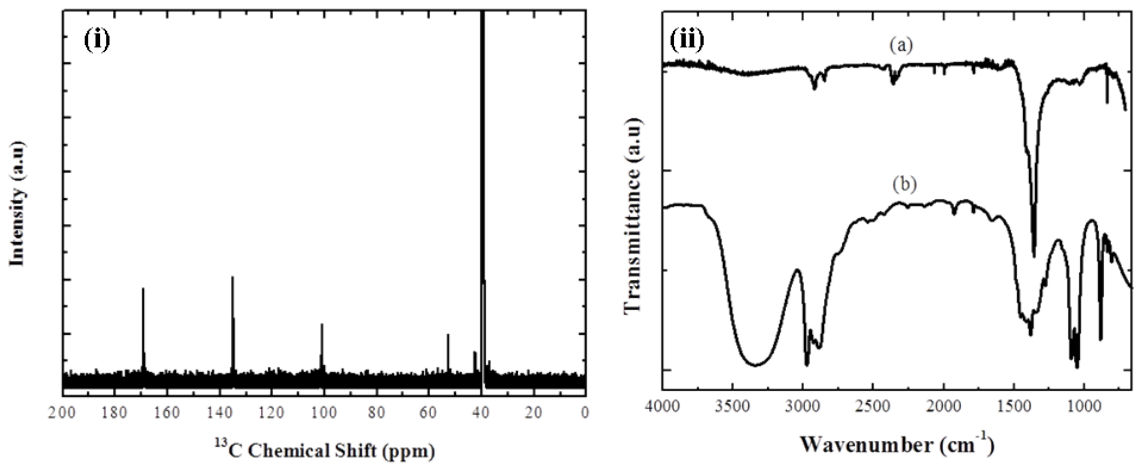

Figure 3. (i) ^{13}C NMR spectrum of C-dots only in D_2O (ii) FTIR of (a) AC and (b) C-dots

Figure 3 (i) shows that the NMR chemical shifts correlating to alkenes in the C-dots are observed between 150 ppm and 120 ppm, while the signals in the range of 200 ppm to 170 ppm correspond to carboxylic acids. There is a small signal at 101 ppm attributed to carbons within an aromatic ring (Ar). Signals observed between 50 and 20 ppm can be assigned to a number of functional groups, including carbons attached to an aromatic ring (Ar-R-C), carbonyl groups, alkanes and unconjugated alkenes. The peak at 51 ppm can be attributed to hydroxyl functionalized carbon. This demonstrates that the C-dots consist of aromatic

carbons which are highly functionalized with carbonyl, hydroxyl and carboxylic acid groups. Similar ^{13}C NMR signals have been previously observed by Tian and co-workers [34].

Figure 3 (i) (a) and (b) shows the FTIR spectra of AC and C-dots, respectively. Both spectra show C-H stretching vibrations (2 bands between 3000 cm^{-1} and 2800 cm^{-1}) and CH_2 bending vibrations (1450 cm^{-1} and between 900 cm^{-1} and 730 cm^{-1}) corresponding to the CH_2 chains in both the activated charcoal and C-dots. However, CH_3 bending at 1380 cm^{-1} is only observed in the spectrum of activated charcoal. Importantly, the C-dots (Figure 2(ii) (b)), show a strong OH stretching vibration attributed to OH groups bound to the C-dot surface, such as phenol groups (Ph-OH), C-OH and COOH groups between 3500 cm^{-1} and 3200 cm^{-1}. C-O stretching vibrations were observed between 1320 cm^{-1} and 1000 cm^{-1} and a weak signal corresponding to C=O was observed at 1720 cm^{-1}. The presence of sp^2 carbons was shown as a strong C=C-H bending vibration between 1000 cm^{-1} and 650 cm^{-1}, alongside stretching and bending vibrations attributed to sp^3 carbons (alkyl chains) between 2900 cm^{-1} and 3000 cm^{-1}. This indicates that the C-dots have a mixture of sp^2 and sp^3 carbon types with Ph-OH, C-OH and COOH functionalities.

Characterization of C-dot/p(DMA) nanocomposites

Raman, XPS, C and H NMR studies of the C-dot structure gave rise to the proposed structure shown in Figure 4 (a). This corresponded well with what literature had proposed where C-dots have been described to have a graphitic core and an oxidised surface. Figure 3 (b) shows the reaction scheme for SIP RAFT polymerization of DMA from the C-dot surface.

By utilizing the C-OH groups decorated on the C-dot surface, Steglich esterification to carboxyl terminated C_{12} CTA to the surface was possible. This was followed by surface initiated RAFT polymerization of DMA monomers to give the C-dot/p(DMA) nanocomposite

(Figure 4 (a)). FTIR spectroscopy, ^{1}H NMR spectroscopy, GPC and TGA were used to monitor this reaction.

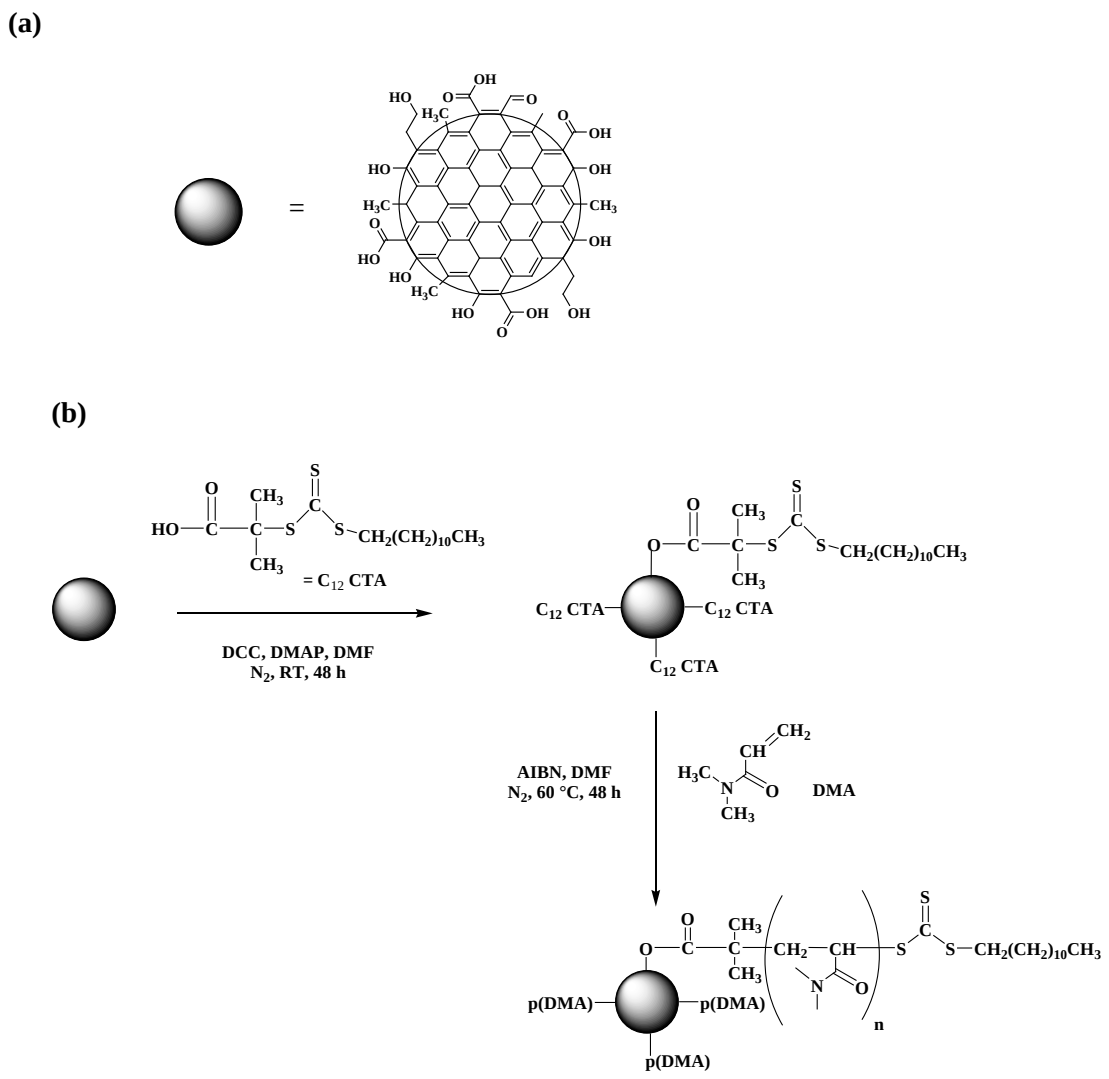

Figure 4. (a) Proposed structure of C-dots (b) reaction scheme for the Steglich esterification between C-dots and the C_{12} CTA and subsequent SIP of DMA via RAFT polymerization.

Figure 5 (a)-(c) shows the FTIR spectra of C-dots, C-dot/C_{12} CTA and C-dot/p(DMA) nanocomposite, respectively. When the C-dots were reacted with the C_{12} CTA the resulting C-dot/C_{12} CTA shows prominent double peaks at 1735 cm^{-1} and 1750 cm^{-1} attributed to the

ester link formed after Steglich esterification. This was indicative that the surface immobilization of the C_{12} CTA was successful. After polymerization of DMA from C-dot/C_{12} CTA the resulting C-dot/p(DMA) nanocomposite is shown in Figure 4 (b) an increased intensity in the C-H stretching vibrations at 3000 cm^{-1} and 2800 cm^{-1}, new C-O stretching vibrations between 1000 cm^{-1} and 1300 cm^{-1}, and acrylamide (C=O) vibrations between 1690 and 1630 cm^{-1} indicates successful grafting-from the C-dot surface. Peaks observed at 1380 cm^{-1} were correlated to CH_3 bending in the DMA functionality.

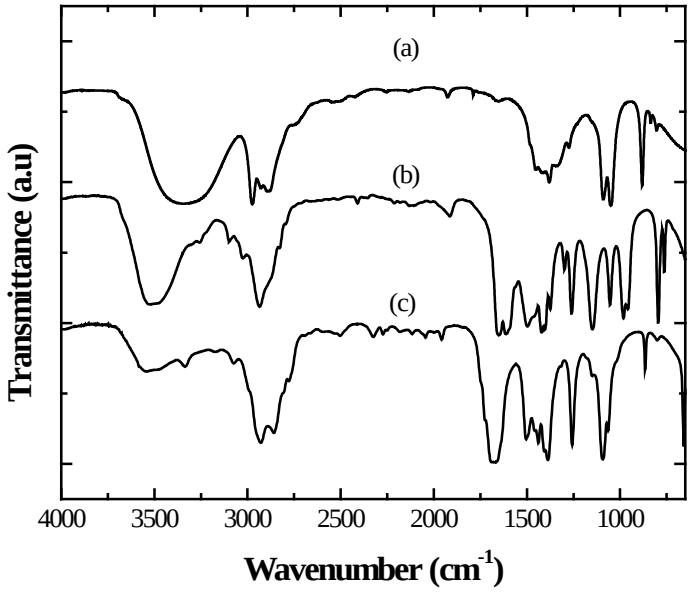

Figure.5. FTIR spectra of (a) C-dots (b) C-dot/C_{12} CTA and (c) C-dot/p(DMA) nanocomposite.

Figure 6 (a)-(d) shows the overlayed thermograms for AC, C-dots, C-dot/C_{12} CTA and C-dot/p(DMA) nanocomposite, respectively. The AC and C-dots (Figure 6 (a) and (b)) did not thermally degrade after heating to 600 °C, shown as no change in mass loss with temperature. Physically adsorbed water and residual DMF was accounted for in the mass loss between 100 °C and 180 °C.

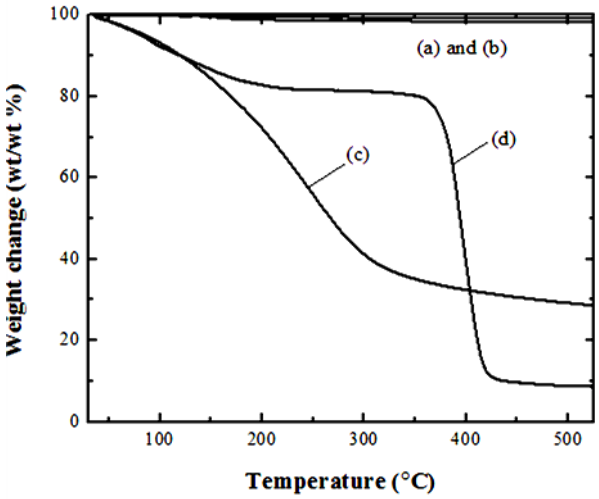

Figure 6. TGA thermograms for (a) AC (b) C-dots, (c) C-dot/C_{12} CTA and (d) C-dot/p(DMA) nanocomposite. At a 10 °C min^{-1} ramp rate under N_2.

The TGA thermograms of the C-dot/C_{12} CTA (Figure 6 (c)) shows a maximum weight change (54 wt/wt %) between 180 °C and 320 °C. This corresponds to the thermal degradation of the C_{12} CTA from the C-dot surface thus leaving a residue of 25 wt/wt % (after heating to 500 °C), which is the C-dot content of the nanocomposite. The TGA thermogram of the C-dot/p(DMA) (Figure 6 (d)) shows a maximum mass loss (72.5 wt/wt %) at higher temperatures between 375 °C and 430 °C, with a residue of 9.8 wt/wt %. This corresponds to the degradation of the RAFT p(DMA) polymer from the C-dot surface.

GPC analysis of p(DMA) cleaved from the C-dot surface revealed the grafted p(DMA) had an Mn of 13 521 g mol-1 and a PDI of 1.13. This was comparable to the values determined via NMR spectroscopy, 14 290 g mol-1 and PDI of 1.15. Given that the diameter of the C-dots was 8.7 nm and assuming that the C-dots are spherical in shape the surface area of the C-dots was calculated to be 237.6 nm2. Therefore the grafting density of the p(DMA) on the C-dot surface was estimated to be 0.338 µmol nm-2.

^{1}H NMR spectroscopy was used to investigate the kinetic control of the surface initiated RAFT polymerizations. Multiple pot reactions were conducted for assigned polymerization

times (t = 0, 1, 4, 8, 12, 24 and 48 h). ^{1}H NMR spectra were then collected and peaks were integrated to determine the concentration of the monomer versus the polymer present at time t. Figure 7 shows the kinetic plot of DMA monomer grafted-from the C-dot/C_{12} CTA via the RAFT process.

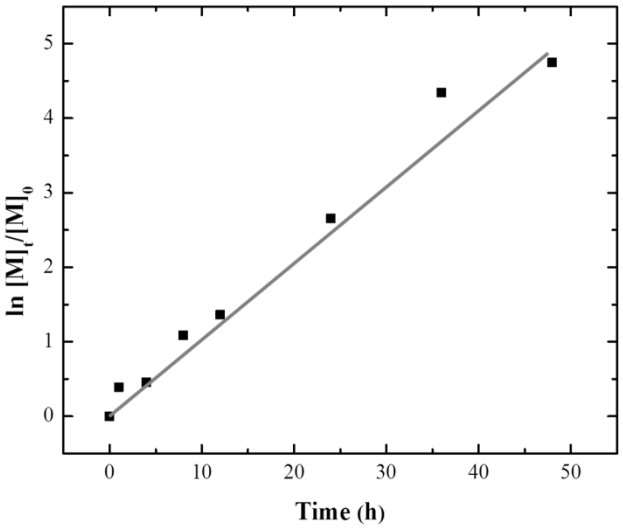

Figure 7. Kinetic plot for the polymerization of DMA grafted from C-dot/C_{12} CTA via RAFT polymerization.

The kinetic plot shows a linear trend (R^2= 0.9792) and follows first order kinetics. Linearity indicates a stead state where the rate of initiation = the rate of termination, resulting in a constant radical concentration. That is the monomer, DMA, is being consumed at a constant rate and is dependent on its initial concentration. This was evidence that polymerization of DMA was controlled via the RAFT process.

Optical properties of the C-dot/p(DMA) nanocomposites

Fundamental to any successful latent fingermark detection reagent is the ability to be able to produce contrast against the surface that the fingermark is deposited on. Figure 8 (a) to (c)

shows the UV-vis absorbance spectra for C-dots, C-dots/C_{12} CTA, and C-dots/p(DMA) nanocomposite in DMF.

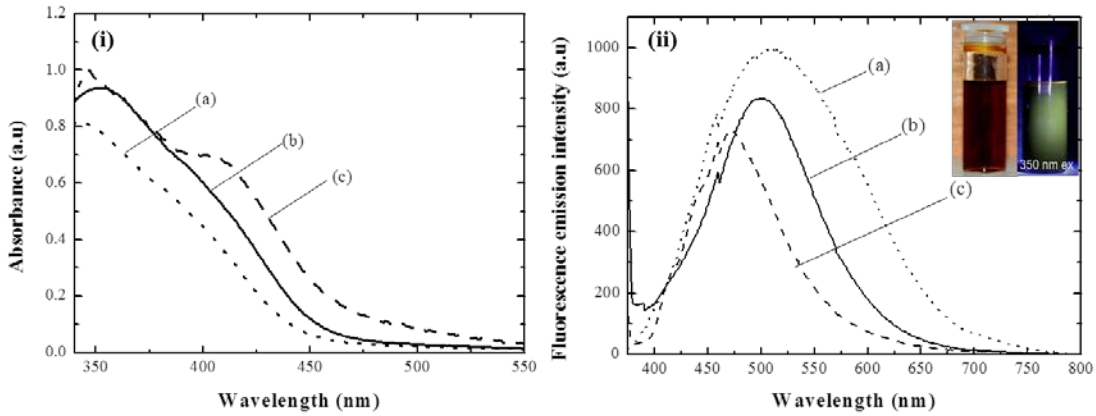

Figure 8. Overlayed (i) UV-vis absorbance spectra and (ii) fluorescence emission spectra of (a) C-dots (b) C-dots/C_{12} CTA and (c) C-dots/p(DMA). Excitation wavelength of 350 nm. Inset: Photograph of C-dots in DMF under white light and UV light illumination (350 nm)

A red-shift in the absorbance shoulder of the C-dots/C_{12} CTA at 422 nm (Figure 8 (i) (b)) when compared to the bare C-dots at 409 nm (Figure 8 (i) (a)) was observed. This was attributed to the attachment of the C_{12} CTA to the C-dot surface, changing the surface properties of the C-dot. After RAFT polymerization of DMA from the C-dot/C_{12} CTA a shoulder appeared between 400 nm and 450 nm. This suggested that the radicals present during RAFT polymerization attacked the C=C groups of the C-dot core further changing the surface properties and hence absorbance spectra profile. Figure 8 (b) shows the fluorescence emission spectra of (i) C-dots (ii) C-dot/C_{12} CTA and (iii) C-dot/p(DMA. The emission spectrum of the C-dots (Figure 8 (b) (i)) shows a broad emission band (FWHM = 167.9 nm). This band is narrowed after surface modification with the C_{12} CTA (FWHM = 104.7 nm, Figure 8 (b)(iii)) and even further narrowed after RAFT polymerization with DMA (FWHM = 94.3 nm, Figure 8 (b) (iii)). This narrowing can be attributed to the alteration of the initial

C-dot surface. As the surface is functionalized with C_{12} CTA, and further with grafting of p(DMA), the quasi-molecular fluorophores on the surface that arise from the carboxylic acid groups [38] are masked. It was also proposed that the OH groups contribute to the optical properties of the C-dots, and consuming these moieties in post-functionalization of the C-dot surface inevitably altered electronic transitions that involved them. The QY of C-dot/p(DMA) nanocomposite was measured against R6G dye to be 24.1 %, which was slightly decreased compared to the precursor C-dot/p(DMA) that had a QY of 28.2 %.

Latent fingermark detection

Latent fingermark development was performed on charged latent fingermarks deposited on non-porous aluminium foil substrates and visualisation under UV light exposure in a dark room. Figure 9 shows latent fingermarks developed on aluminium foil by the C-dot polymer nanocomposites and photographed under UV light (350 nm setting on the Polilight®). The photographs are also arranged into columns corresponding to capture modes (left to right) with no filter, a green filter (555 ± 24 nm) and a red filter (640 ± 40 nm). The developed fingermarks in each column are shown in pairs where fingermarks on the left were developed "fresh" (within 2 hours of latent fingermark deposition onto the substrate) are "aged" (2 weeks after latent fingermark deposition onto the substrate).

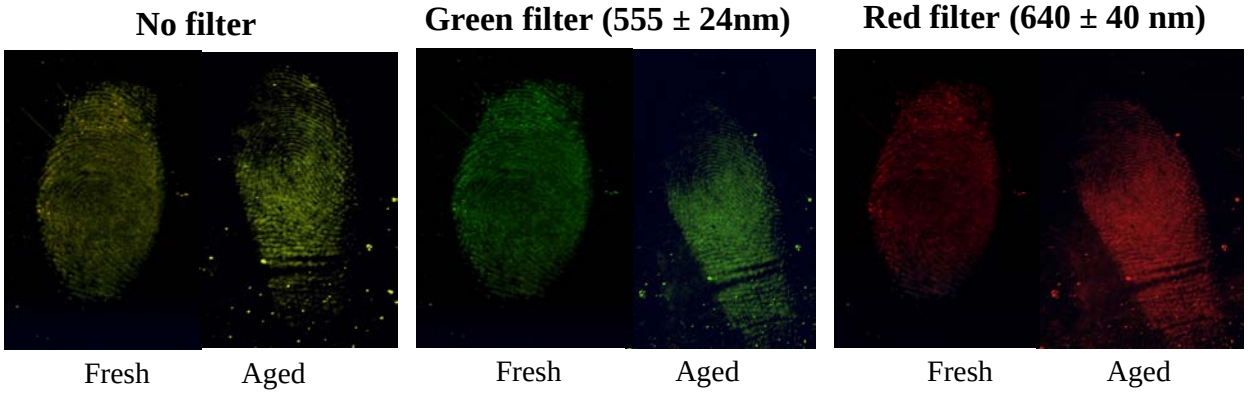

Figure 9. Latent fingermarks on aluminium foil developed by row C-dot/p(DMA) solution reagent. Photographs were taken under UV illumination (350 nm) using no filter, a green filter (555 ± 24 nm) and a red filter (640 ± 40 nm) as annotated. Left fingermark: fresh latent fingermarks, right fingermark: aged fingermarks.

The C-dot/p(DMA) solution reagent showed preferential adherence to the latent fingermark over the aluminium foil substrate. Photographs taken with no filter showed that the C-dot/p(DMA) nanocomposite (dried on the latent fingermark) appeared lime green under UV-illumination which agreed with its fluorescence emission spectra (fluorescence emission maximum at 473.3 nm). The photographs captured with the green and red filter showed the latent fingermark developed had good contrast in these respective colours.

CONCLUSION

C-dots were synthesized via a hydrothermal route (reflux under acidic conditions). The surface of C-dots was characterized using Raman, FTIR, ^{13}C NMR and XPS spectroscopies. These studies revealed that the C-dots have an aromatic carbon core (sp^2 carbon) with an oxidized surface containing C-OH and COOH moieties. These oxidized surface moieties contributed to the optical properties of the C-dots. The OH moieties were used to functionalize the C-dot surface with a C_{12} CTA enabling the surface initiated RAFT polymerization of a DMA monomer to produce C-dot/p(DMA). The C-dot/p(DMA) nanocomposite was water soluble and hence used as an aqueous solution for latent fingermark detection. Latent fingermarks deposited on non-porous substrates, aluminium foil were successfully detected with significant visual contrast provided by the luminescent, non-toxic, aqueous C-dot/p(DMA) nanocomposite reagent.

ACKNOWLEDGEMENTS

We would like to thank the South Australian Department of Justice for project funding. The authors also acknowledge the Australian Microscopy and Microanalysis Research Facility (AMMRF) at the School of Chemical and Physical Sciences, Flinders University.

REFERENCES

1 Menzel ER, Savoy SM, Ulvick, SJ, Cheng KH, Murdock RH and Suduth MR, *J Forensic Sci* **45**:545 (2000).

2 Menzel ER, Takatsu M, Murdock RH, Bouldin K and Cheng KH, *J Forensic Sci* **45**:770 (2000).

3 Feng G, Jiaxing H, Jun Z, Qun L, Xiufeng S and Jincheng Z, *Nanotechnology* **22**:75705 (2011).

4 Dilag J, Kobus H and Ellis AV, *Forensic Sci Int* **187:**97 (2009).

5 Jin Y, Luo Y, Li G, Li J, Wang Y, Yang R and Lu W, *Forensic Sci Int* **179**:34 (2008).

6 Dilag J, Kobus H, and Ellis AV, *Forensic Sci Int* **228**:105-114 (2014).

7 Algarra M, Jiménez-Jiménez J, Miranda MS, Campos BB, Moreno-Tost R and Rodriguez-Castellón E, *Surf Interface Anal* **45**:612 (2012).

8 Algarra M, Jiménez-Jiménez J, Moreno-Tost R, Campos BB and Esteves da Silva JCG, *Opt Mater* **33**:893 (2011).

9 Alivisatos AP, *Science* **271**:933 (1996).

10 Derfus AM, Chan WC and Bhatia SN, *Nano Lett* **4**:11 (2004).

11 Fogg DE, Radzilowski LH, Dabbousi BO, Schrock RR, Thomas EL and Bawendi MG, *Macromolecules* **30**:8433 (1997).

12 Allam A and Sarkar S, (PVN: US20110217721 A1) USA PATENT (2010).

13 Anilkumar P, Wang X, Cao L, Sahu S, Liu J-H and Wang P, *Nanoscale* **3**:2023 (2011).

14 Baker SN and Baker GA, *Angew Chem Int ed* **49**:6726 (2010).

15 Callan JF, Fowley CP, McCaughan B and Devlin A, *Chem Comm* **48**:9361 (2012).

16 Chandra S, Pathan SH, Mitra S, Modha BH, Goswami A and Pramanik P, *RSC Advances* **2**:3602 (2012).

17 Kwon W and Rhee S-W, *Chem Comm* **48**:5256 (2012).

18 Li X, Wang H, Shimizu Y, Pyatenko A, Kawaguchi K and Koshizaki N, *Chem Comm* **48**:932 (2011).

19 Sun Y-P, Luo PG, Sahu S, Yang S-T, Sonkar SK and Wang J, *J Mater Chem B* **1**:2116 (2013).

20 Sun YP, Zhou B, Lin Y, Wang W, Fernando KA and Pathak P, *J Am Chem Soc* **128**:7756 (2006).

21 Sun YP, Wang X, Lu F, Cao L, Meziani MJ and Luo PG, *J Phys Chem C* **112:** 18295 (2008).

22 Cao L, Wang X, Meziani MJ, Wang H, Luo PG and Lin Y *J Am Chem Soc* **129**:11318 (2007).

23 Wang Q, Zheng H, Long Y, Zhang L, Gao M and Bai W, *Carbon* **29:**3134 (2011).

24 Qiao Z-A, Wang Y, Gao Y, Li H, Dai T and Liu Y, *Chem Comm* **46**:8812 (2010).

25 Ray SC, Saha A, Jana NR and Sarkar R, *ACS Nano* **6**:400 (2009).

26 Sahu S, Behera B, Maitib TK and Mohapatra S, *Chem Comm* **2**:8660 (2012).

27 Wang F, Pang S, Wang L, Li Q, Kreiter M, and Liu C, *Chem Mater* **22**:4528 (2010).

28 Wohlgemuth S, White R and Titirici M, *Carbon* **1**:1-4 (2010).

29 Yang Y, Cui J, Zheng M, Hu C, Tan S and Xiao Y, *Chem Comm* **48**:380-382 (2012).

30 Zhao Q-L, Zhang Z-L, Huang B-H, Peng J, Zhang M and Pang D-W, *Chem Comm* **41**:5116 (2008).

31 Liu J-H, Yang S-T, Chen X-X and Wang H, *Cur Drug Metabolism* **13:**1046 (2012).

32 Palashuddin SK, Amit J, Anumita P, Ghosh SS and Chattopadhyay A, *Scientific Reports* **2** (2012).

33 Ray SC, Saha A, Jana NR and Sarkar R, *ACS Nano* **6**:400 (2009).

34 Tian L, Ghosh D, Chen W, Pradhan S, Chang X and Chen S, *Chem of Mater* **21**:2803 (2009).

35 Ferrari A and Robertson J, *Phy Rev B* **61**:14095 (2000).

36 Escribano R, Sloan JJ, Siddique N, Sze N and Dudev T, *Vib Spec* **26**:179 (2001).

37 Krishnan KS and Guha AC, *Proc Indian Acad Sci* **1**:242 (1934).

38 Zangmeister CD and Pemberton JE, *J Phys Chem A* **105**:3788 (2001).

39 Galande C, Mohite AD, Naumov AV, Gao W, Ci L, and Ajayan A *Scientific Reports* **1** (2011).